A Study on Numerical Analysis of Stress Distribution for Thermal Nanoimprint Lithography Process

Bum-Goo Cho, Soon-Yeol Park, Seung-Su Yang and Taeyoung Won

Department of Electrical Engineering, School of Information Technology Engineering,
Inha University, Incheon, Korea, twon@hsel.inha.ac.kr

Abstract

We investigated the deformation of the viscoelastic polymethyl methacrylene (PMMA) resist wherein a rigid SiO2 stamp with a rectangular line pattern is imprinted for thermal nano-imprint lithography (NIL). We calculated the stress distribution in the polymer resist during the molding process by finite element method (FEM). Our simulation results revealed asymmetric von Mises stress distribution for the polymer around the external line, which is due to the squeezing flow under the flat space. The stress seems to concentrate at the sidewall which is close to the centerline of the whole structure. Our simulation revealed that micro gap is formed between the replicated structure and the outer wall of the mold.

Keywords: stress distribution, thermal nano-imprint lithography, viscoelastic, Polymethyl methacrylene resist, von Mises stress

I. INTRODUCTION

One of the most important micro/nanofabrication technologies is lithography, which transforms micro/nano-scale patterns to certain substrate, such as silicon, metal, and polymer. Conventional lithographic methods, such as electron beam lithography, focused ion beam lithography, optical projection lithography, extreme UV lithography and X-ray lithography, have been widely used in the fabrication of nano-scale devices. However, there are a lot of issues yet to be resolved in these methods. The cost of these conventional lithographic methods is also extremely high for most potential applications [1].

In this sense, nano-imprint lithography (NIL) is one of the most promising techniques for pattern transfer. NIL relies on a direct mechanical deformation of the resist material and can therefore achieve resolutions beyond the limitations which are set by a light diffraction or a beam scattering. It enables both high resolution up to sub-25 nm which is not accomplishable in photolithography and fast throughput compared to serial processing methods such as electron beam or scanning probe microscopy (SPM) lithography, so it is expected as an alternative lithography method to conventional ones [2]. In addition, NIL is expected to realize a low cost and high-throughput production. In the thermal NIL process, a high speed imprinting was reported such as a role-to-role imprint. In order to improve the NIL technology, it is essential to understand the deformation behavior of polymer during the imprinting process. Success of the pattern transfer in NIL depends on exact deformation of a polymer resist according to stamp patterns and clear separation of a stamp from a polymer resist [3].

Despite the prospective potential for nano-scale pattern transfer, there are few literature publications on the numerical modeling on NIL processes [4-6]. The goal of this study is to study the mechanical behavior of imprinted polymer resist during molding in thermal imprint lithography. Basic rules of stress distribution and evolution were extracted from the results of finite element method (FEM) simulation and explained in the light of viscoelastic property of Polymethyl methacrylene (PMMA).

In this work, we modeled the NIL process and employed commercially available software, COMSOL Multiphysics, for the implementation of our model. In this paper, we report the stress distribution of the polymer deformation process on the imprinting pressure.

II. SIMULATION METHODOLOGY

In this computational study, an implicit algorithm was employed for solving the following governing equations. [7]

The continuity equation

$$\frac{\partial \rho}{\partial t} + \rho \frac{\partial u_i}{\partial x_i} = 0 \tag{1}$$

The Navier-Stokes momentum equation

$$\frac{\partial u_i}{\partial t} + u_j \frac{\partial u_i}{\partial x_j} = \frac{1}{\rho} \frac{\partial}{\partial x_j} \sigma_{ij}(u) + f_i \tag{2}$$

Where $\sigma_{ij} = -p\delta_{ij} + 2\mu d_{ij}$, $d_{ij} = \frac{1}{2}\left(\frac{\partial u_i}{\partial x_j} + \frac{\partial u_j}{\partial x_i} \right)$, i = 1, 2, 3 and j = 1, 2, 3.

In these equations, t is the time, u_i is the velocity component in x_i , ρ is the density, μ is the dynamic viscosity, f_i is the body force component in x_i and σ_{ij} , d_{ij} denote the stress and strain tensors, respectively.

Strain-displacement equation

Strain-displacement equations describe the basic relations between displacement and strain.

$$\varepsilon_x = \frac{\partial u_x}{\partial x} \tag{3-a}$$

$$\varepsilon_y = \frac{\partial u_y}{\partial y} \tag{3-b}$$

$$\varepsilon_z = \frac{\partial u_z}{\partial z} \tag{3-c}$$

$$\gamma_{xy} = \frac{\partial u_x}{\partial y} + \frac{\partial u_y}{\partial x} \tag{4-a}$$

$$\gamma_{yz} = \frac{\partial u_y}{\partial z} + \frac{\partial u_z}{\partial y} \tag{4-b}$$

$$\gamma_{zx} = \frac{\partial u_z}{\partial x} + \frac{\partial u_x}{\partial z} \tag{4-c}$$

Where ε and γ are the normal strain and shearing strain.

Strain compatibility equation

Strain compatibility equation is based on the consideration of the continuum assumption. When we analyze the strain-displacement behavior, we must ensure the continuity of material before and after deformation. [8]

$$\frac{\partial^2 \varepsilon_x}{\partial y^2} + \frac{\partial^2 \varepsilon_y}{\partial x^2} + \frac{\partial^2 \gamma_{xy}}{\partial x \partial y} \tag{5-a}$$

$$\frac{\partial^2 \varepsilon_y}{\partial z^2} + \frac{\partial^2 \varepsilon_z}{\partial y^2} + \frac{\partial^2 \gamma_{yz}}{\partial y \partial z} \tag{5-b}$$

$$\frac{\partial^2 \varepsilon_z}{\partial x^2} + \frac{\partial^2 \varepsilon_x}{\partial z^2} + \frac{\partial^2 \gamma_{zx}}{\partial z \partial x} \tag{5-c}$$

$$2\frac{\partial^2 \varepsilon_x}{\partial y \partial z} = \frac{\partial}{\partial x}\left(-\frac{\partial \gamma_{yz}}{\partial x} + \frac{\partial \gamma_{xz}}{\partial y} + \frac{\partial \gamma_{xy}}{\partial z} \right) \tag{6-a}$$

$$2\frac{\partial^2 \varepsilon_y}{\partial x \partial z} = \frac{\partial}{\partial y}\left(\frac{\partial \gamma_{yz}}{\partial x} - \frac{\partial \gamma_{xz}}{\partial y} + \frac{\partial \gamma_{xy}}{\partial z} \right) \tag{6-b}$$

$$2\frac{\partial^2 \varepsilon_z}{\partial x \partial y} = \frac{\partial}{\partial z}\left(\frac{\partial \gamma_{yz}}{\partial x} + \frac{\partial \gamma_{xz}}{\partial y} - \frac{\partial \gamma_{xy}}{\partial z} \right) \tag{6-c}$$

In summary, to obtain the stress distribution by finite element method (FEM), firstly, the force load is transferred to strain load, then displacement load by constitutive equation and strain-displacement equation, respectively. Then, the continuity equations and strain compatibility equations are solved by finite element method (convert differential equation to linear equation group) and we calculate the displacement for each element. Finally, the strain and stress for each element are derived from displacement data by strain-displacement equation and constitutive equation in sequence.

NSTI-Nanotech 2009, www.nsti.org, ISBN 978-1-4398-1784-1 Vol. 3, 2009

III. SIMULATION RESULTS AND DISCUSSION

Figure 1 is a schematic diagram illustrating the physical model for imprinting process. The mold has five line patterns with 800 nm wherein the width is 50 nm and the height is 50 nm. Each line pattern is at interval of 50 nm. The polymer materials we employed in our simulation were PMMA and the imprint temperature was 140℃. The SiO2 mold was modeled as a rigid body, and the PMMA resist was modeled as a visco-elastic material. Table 1 shows the material constants used for our numerical analyses. The pressure of 50 MPa was applied on the top of the mold and kept constant for various time periods during pressing process. After the pressing process, PMMA specimens were quickly cooled down so that the specimens almost preserve the shape at the end of the pressing process.

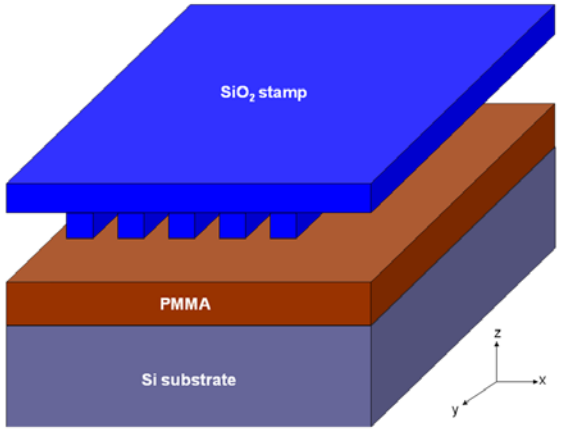

Fig. 1. Schematic diagram illustrating the physical model.

Table 1. Material constants of PMMA resist.

Material constant	Value
Young's modulus	3 GPa
Poisson's ratio	0.4
Heat capacity	1420 J / K
Thermal expansion coefficient	7.0 10^{7} K^{-1}
Thermal conductivity	0.19 W / (m K)
Density	1190 kg / m^{3}

The simulated 3-dimensional profile of stress distributions on the polymer are shown in Figure 2. The contour of simulated results represents the residual von Mises stress. The major cause of the residual von Mises stress is the thermal shrinkage in cooling process uniformly. The nonuniformity of the residual von Mises stress is caused by the distribution of viscous strain at the end of the pressing process.

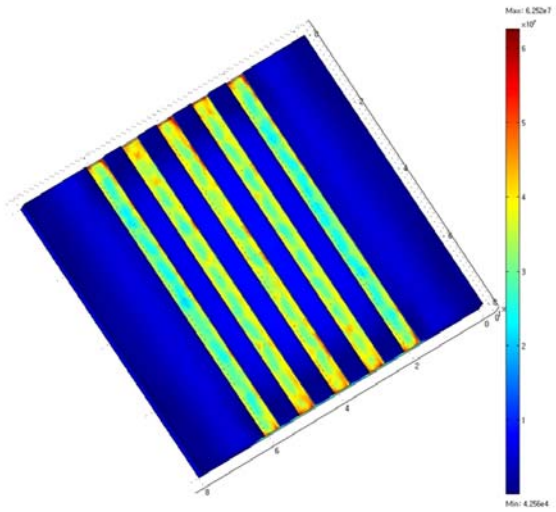

Fig. 2. Simulated 3-dimensional profile of stress distribution on the polymer.

Figures 3(a), 3(b) and 3(c) are cross-sectional profiles of von Mises stress distribution of the polymer on x-y, y-z and z-x plane, respectively. These calculated results exhibits asymmetric von Mises stress distribution of the polymer around the external line caused by the squeezing flow under flat space. Referring to Figures 3(a), 3(b), and 3(c), we can see that the local stress reaches maximum near each contact interface, from symmetric centerline to the edge. Similarly, the stress concentrates locally both at the corner of transition zone between the replicated patterns and residual layer. However, different highest local stress values are revealed depending on the relative distance to the symmetric centerline.

Considering a certain micro cavity which is located away from the symmetry center, our simulation result shows that both sides of the walls of the micro cavity are highly stressed. The stress is concentrated at the sidewall close to the centerline of the whole structure and micro gap was formed between the replicated structure and the outer wall of the mold.

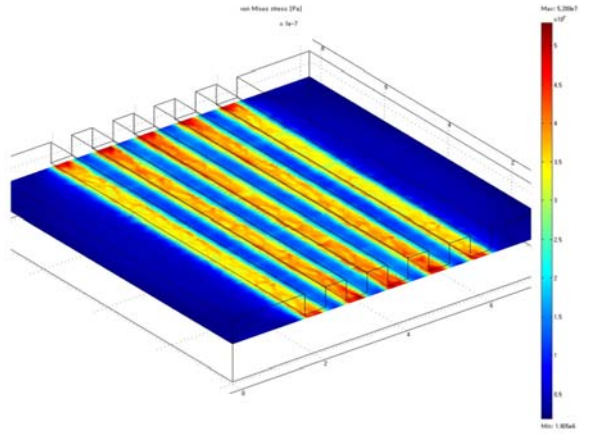

(a)

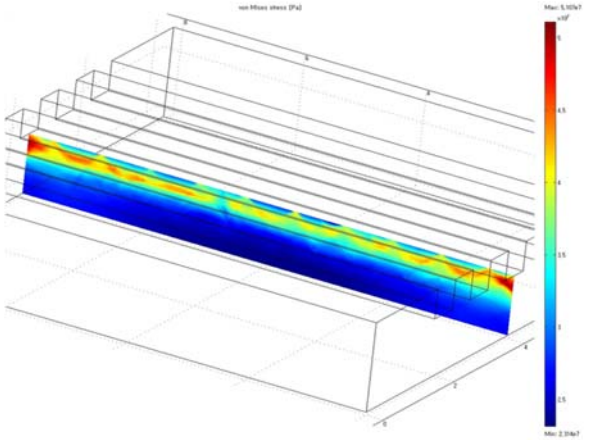

(b)

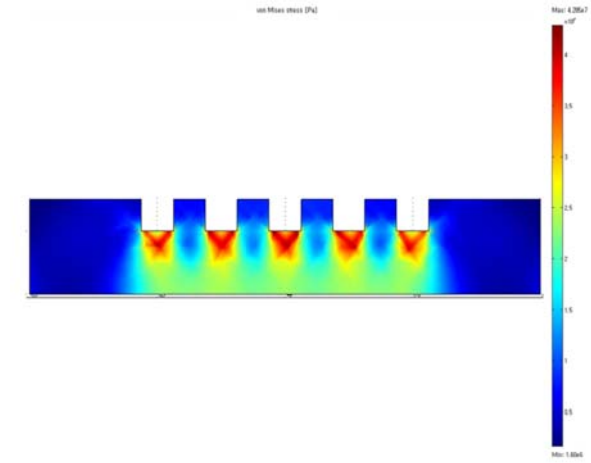

(c)

Fig. 3. Simulated cross-section profile of von Mises stress distribution: (a) x-y plane, (b) y-z plane, (c) z-x plane.

IV. CONCLUSION

We proposed a numerical model for imprinting a rigid SiO_2 stamp into a visco-elastic polymer resist, which is essential for simulating the pattern transfer and for figuring out its related phenomena in thermal NIL. The behavior of polymer deformation was investigated in detail by means of stress distribution analysis. In the imprint process, significant compressive stress was found to be generated under the stamp pattern due to the compression of the polymer resist, which causes the polymer to flow and to fill the cavity of the stamp for both patterns. Our simulation results imply that the FEM simulation will make possible the theoretical prediction of the de-molding process as well as determination of a range of process parameters which will allow the successful de-molding even at the stage of a process design in an economical and reliable manner.

ACKNOWLEDGEMENT

This research was supported by the Ministry of Knowledge Economy, Korea, under the ITRC (Information Technology Research Center) support program supervised by the IITA (Institute of Information Technology Advancement) (IITA-2008-C109008 010030) and the authors would like to acknowledge the support from KISTI Supercomputing Center (KSC-2008-S03-0003).

REREFENCES

[1] Chen. Y and A. Pepin, Electrophoresis, 22(2), 187 (2001).

[2] Stephen Y. Chou, Peter R. Krauss, and Preston J. Renstrom, Science 272, 85 (1996).

[3] L. J. Guo and J. Phys. D: Appl. Phys. 37, R123 (2004).

[4] H. D. Rowland, A. C. Sum, P. R. Schunk, and W. P. King, J. Micromech. Microeng., 15 (2005).

[5] T. Eriksson and H. K. Rasmussen, J. Non-Newtonian Fluid. Mech., 127 (2005).

[6] Y. Hirai, S. Yoshida, T. Kanakugi, and T. Konishi, J. Vac. Sci. Technol., B22 (2004).

[7] Jun-Ho Jeong, Youn-Suk Choi, Young-Jae-Shin, Jae-Jong Lee, Kyoung-Taik Park, Eung-Sug Lee, and Sang-Rok Lee, Fibers and Polymers, Vol. 3, No. 3, 113 (2002).

[8] Marc Baus and Ronald Lovett, Phys. Rev. Lett, 65, 1781 (1990).